*Steel and Composite Structures, Vol. 8, No. 3 (2008) 243-264*
DOI: http://dx.doi.org/10.12989/scs.2008.8.3.243



# Experimental investigation of the behaviour of a steel sub-frame under a natural fire

Aldina Santiago† and Luís Simões da Silva†

*ISISE - Department of Civil Engineering, University of Coimbra, Coimbra, Portugal*

Gilberto Vaz‡

*Department of Mechanical Engineering, ISEC - Polytechnic Institute of Coimbra, Coimbra, Portugal*

Paulo Vila Real‡†

*LABEST - Department of Civil Engineering, University of Aveiro, Aveiro, Portugal*

António Gameiro Lopes‡‡

*Department of Mechanical Engineering, University of Coimbra, Coimbra, Portugal*

*(Received December 1, 2008, Accepted June 3, 200)*

**Abstract.** This paper details a testing facility ("NATURAL FIRE FACILITY") that allows closely-controlled experimental testing on full-scale sub-frames while reproducing the spatially transient temperature conditions measured in real fires. Using this test facility, an experimental investigation of six steel sub-frames under a natural fire was carried out at the Department of Civil Engineering of the University of Coimbra. The main objective of these tests was to provide insight into the influence of these connection types on the behaviour of steel sub-structures under fire. The experimental layout is defined by two thermally insulated HEA300 columns and an unprotected IPE300 beam with 5.7 m span, supporting a composite concrete slab. Beam-to-column connections are representative of the most common joint type used on buildings: welded joints and extended, flush and partial depth plate. Finally, the available results are presented and discussed: evolution of the steel temperature; development of displacements and local deformations and failure modes on the joints zone.

**Keywords :** structural engineering; steel and composite structures; fire behaviour; full-scale tests; structural integrity

## 1. Introduction

The study of any aspect of the behaviour of a structure always starts from observations of the behaviour of physical models, either from carefully planned and executed experiments or uncontrolled

†Lecturer, Corresponding author, E-mail: aldina@dec.uc.pt

accidents. This is also true for the behaviour of urban constructions in fire. Whilst observations from accidental fires in structures can lead to qualitative speculations of the possible behaviour of structures under fire attack, more precise and quantitative understanding can only be obtained from carefully planned and conducted experimental studies (Wang 2002).

Current fire testing devices are usually built with a high degree of isolation to avoid thermal losses and although they allow controlled variations of temperature with time, they are normally only able to provide near-uniform temperature condition inside its enclosure. In addition, the size of the specimens is usually limited, preventing the testing of substructures. However, real fires are characterized by a spatial and time variation of the temperature throughout the structure, as was recently observed in the fire tests at Cardington (Wald *et al*. 2006). Failure to reproduce their real thermal conditions in a fire test means that the critical failure mode may be overlooked and lead to wrong and maybe unsafe conclusions. This was already demonstrated by other authors, such as the ECSC project 7210-PA/PB/PC/PD/PE/PF/PR-060 **(*ECSC 7210 2000*)**, where the value of using real fire curves instead of the usual ISO curve was developed.

The behaviour of steel joints under fire loading was precisely one such case. In fact, as recently as 1995, the European pre-standard on the fire response of steel structures (CEN 1995) deemed it unnecessary to assess the behaviour of steel joints under fire conditions. This approach was supported by the argument of the increased massivity of the joint area. In reality, joints may fail and against common belief, during the cooling phase of natural fire, as was predicted by Santiago *et al*. (2003) and observed during the fire test in Cardington (Wald *et al*. 2006).

It is the objective of this present paper: (i) to describe an experimental investigation of six steel sub-frames under a natural fire that was undertaken at the Department of Civil Engineering of the University of Coimbra, Portugal, to provide insight into the influence of these connection types on the behaviour of steel sub-structures under fire; and (ii) to detail the development of a unique fire testing facility ("NATURAL FIRE FACILITY") that allows closely-controlled experimental testing on full-scale sub-frames while reproducing the spatially transient temperature conditions measured in real fires.

## 2 Existing fire testing devices

Several facilities are currently used for the fire testing of structures; some of them are reviewed here for comparison with the present "Natural Fire Facility". These facilities could be divided according to different classifications: by heat sources, by use, by method of handling material, by recirculation, by heat recovery. Here they are classified as: i) closed facilities (furnaces) and ii) open facilities. Selection of a specific facility to use depends on the geometry and dimensions of the tested structure. For the furnaces two types of heat sources may be used: combustion of fuel (fuel-fired furnaces and oil-fired furnaces) and conversion of electrical energy to heat (electrical furnaces). For economic reasons, *fuel-fired furnaces* are the most widely used (Trinks *et al*. 2004).

In fuel-fired furnaces, the specimens to be tested may make a difference in the furnace design; two types of furnaces may be designed: standard and research furnaces. Standard furnaces are used to test constructional elements according to standard tests (Fig. 1). These furnaces have normalized dimensions and are usually classified as vertical, horizontal, column furnaces and combi-furnaces. Vertical furnaces are used for testing of primarily vertically oriented elements of construction e.g. walls, doors, partitions, glazing, facades, ducts etc. Horizontal furnaces are used for the testing of primarily horizontally oriented elements of construction e. g. timber and concrete floors, decks, mezzanine floors, ducts etc.; they are

Fig. 1 Vertical furnace at the University of Aveiro, Portugal

also widely used to test fire protection to structural steel work. Column furnaces are vertically oriented furnaces for testing of columns by providing four sided exposure. Finally combi-furnaces are combinations of vertical and horizontal furnaces. Research furnaces are focused on tests of structural elements and their dimensions and conditions are defined according to the tested specimen (Fig. 2).

The basic elements of a furnace box are: a) the heat-resistant lining with insulation, b) the steel-supporting structure and casing, c) the heat-releasing, distributing, and control equipment, including circulation of hot gases and provision for waste gas discharge; and d) load-holding and load-handing equipment. Fuel and air enter the furnace through burners that fire through refractory tiles. The combustion gases circulate over the inside surfaces of the walls, ceiling, hearth and specimen, heating all by radiation and convection. Usually, in research furnaces, and in order to expose the specimen to uniform heating and to prevent direct exposure to the flame itself, the furnace box is partially divided by a partition, the specimen is located within one chamber while the gas burner is fixed in the other as shown in Fig. 2 (Liu *et al*. 2002).

*Electrical furnaces* use resistances to process heating. They usually involve high electricity costs, and may require circulating fans to ensure that temperature uniformity is achieved by the flow motion of the

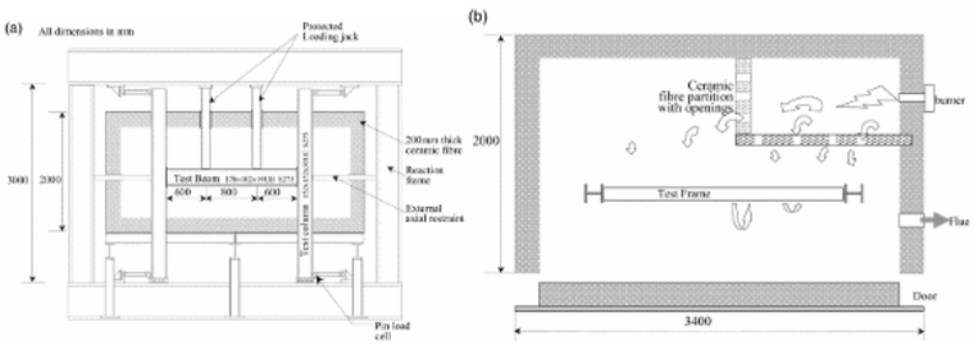


Fig. 2 Research furnace. a) Testing assembly (elevation) b) Top view: section through furnace (Liu *et al*. 2002)

Fig. 3 Electrical furnaces at the University of Coimbra, Portugal

products of combustion in combustion fuel devices (Fig. 3). The range of geometries is similar to those presented for fuel-fired furnaces.

The fact that the test procedures and results obtained from furnaces are normalized increases the usefulness of theses devices for engineering calculations; however their are not very effective in developing our understanding of realistic structural behaviour in fire: they are not able to reproduce i) a "natural" cooling of the heated structure and ii) temperature gradient across the specimen span and cross-section, moreover, tests on real sub-structures are limited due to the limitations on the furnace sizes.

Open facilities consist of mats that surround the specimen to be heated; they have the advantage of being easily adapted to heating localized areas or long specimens; temperature gradient is also possible, however natural cooling is not reproduced and neither are flames similar to those observed in urban fires. Two types of mats can be used: a) electroceramic mat elements, b) induction heating.

*Electroceramic mat elements* (Vila Real *et al*. 2003) include: small ceramic resistances, a power

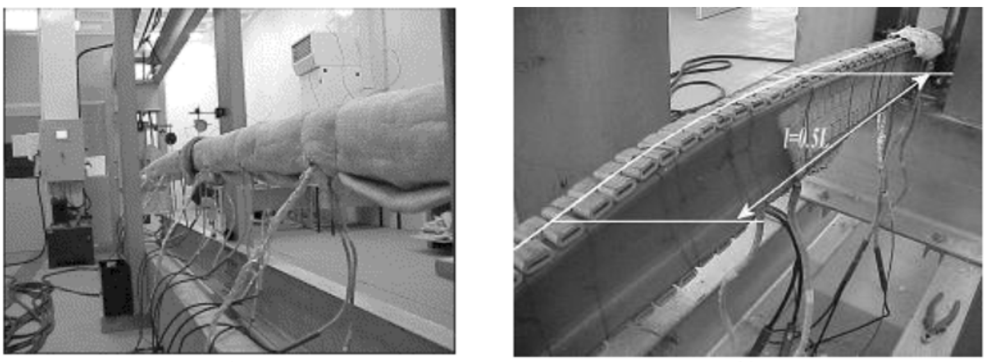

a) b)

Fig. 4 a) Testing assembly of a steel beam, b) electroceramic mat elements (Vila Real *et al*. 2003) system and a control system. The ceramic resistances have low electrical power and are heated through the power system by a three-phase transformer, hand or automatically operated. To manage the temperature, the control system defines a fire curve with linear heating, maximum temperature and period, and a linear cooling. Control of separated ceramic resistances ensures a uniform heating along the length of the specimen to be heated. The thermal efficiency is improved by using a ceramic fibre blanket to insulate the specimen and the electroceramic mat (Fig. 4).

In *induction heating*, a current passes through a coil that surrounds the specimen to be heated and the electric current frequency to be used depends on the mass of that element. The induction coil must be water cooled to prevent overheating. Induction heating usually uses less electricity than resistance heating.

## 3. Design of the "Natural Fire Facility"

### 3.1 Introduction and objectives

In order to solve some problems inherent in the previous fire testing devices, the "Natural Fire Facility" was developed. The main goals of this design were: i) to provide a transient regime with controlled heating and cooling phases, ii) to ensure versatility to test any kind of geometry or dimensions of the tested structure, iii) to divide the tested structure in several zones and to specify individual thermal load strategies to each zone, iv) to provide temperature gradient within the structural cross-section. An additional goal is the possibility to simulate loading conditions similar to those observed in a real structure under a fire, so, the applications of different types of mechanical loading are also considered.

### 3.2 Heating equipment

This heating system is constituted by individual gas burners suspended along the specimen to be heated. Each of these burners has 0.5 m of length and different thermal loads can be applied for each of them (Fig. 5). The burners are fed by propane gas through flexible copper pipes (to allow adjustments at the support structure) and are supplied by a battery of gas reservoirs located outside the Test Laboratory

Fig. 5 a) Individual gas burner; b) Heating system


Fig. 6 Battery of gas reservoirs

(Fig. 6). Propane gas allows a definition of a yellow turbulent diffusion flame, common in urban fires. The burners were designed and developed in collaboration with CHAMA S.A.

In order to reduce the heat losses to the surroundings and the air entrainment to the vicinity of the heated specimen, rockwool panels are fixed vertically from the exhaust system to the floor. The internal face of the rockwool was aluminized to reflect radiation (Fig. 13). This way, the specimen heated up not only because of direct incidence of flames but also through radiation from flames, and from the exhaust system and rockwool panels.

### *3.3 Control system*

An external control system was applied to regulate individually each specimen zone with one or more burners, and to allow to specify the gas delivered to the system and thus to achieve the thermal load strategy. The control system as well as the gas and electrical circuits are illustrated in Fig. 7. Each control system is constituted by the following items: i) a control box IFS 258 (Fig. 7b), ii) a KS 90 programme, iii) gas reservoirs and iv) several valves. The sequence of the control system operations is described next.

#### *3.3.1 Start up*

The start-up of the control system is divided into two sequential times: first the ignition of the pilot burners (two in each zone) and second the ignition of the heat burners of the corresponding zones. The start-up operations of one control system will be briefly described.

The first step on the ignition of the burners is to switch on the automatic burner control unit, IFS 258. After that, the control box IFS 258 was carried out a test for flame simulation and failsafe operation. If a flame is detected before the burners ignite, the burner control starts the flame simulation delay time. If the flame simulation is extinguished during this time, the pilot burner will ignite; otherwise the control box IFS 258 will indicate a fault. If no flame sign is detected during the test, the control box IFS 258 will open the valves on the gas circuit and ignite the first pilot burner.

Afterwards, if pilot ignition is not burning, an automatic restart is tried, but if after the second try and the flame is still not detected, fault lock-out takes places, i.e. the valve closes and the alarm is switched

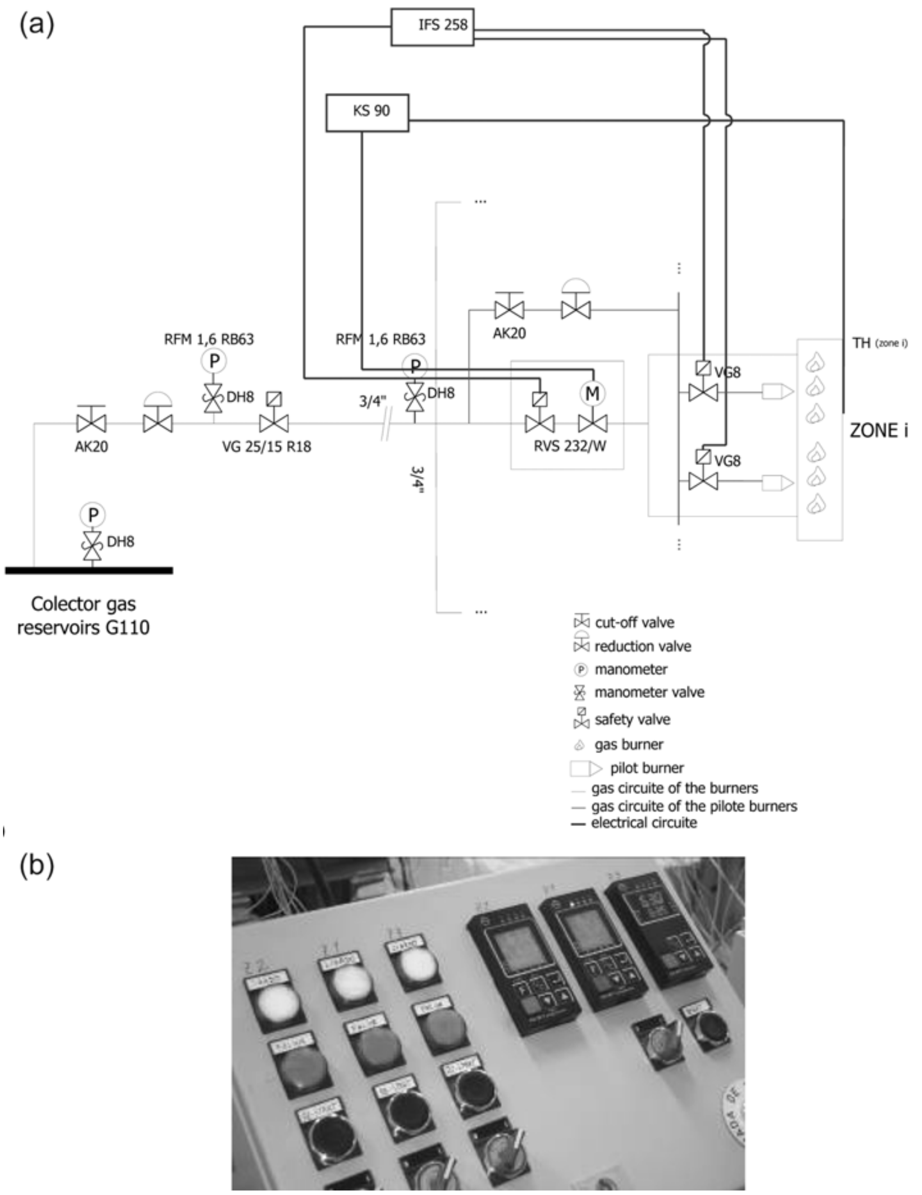


Fig. 7 Temperature control system: a) control system operation, b) control box IFS 258

on. However, if flame is detected during ignition, the start-up of the pilot burner is concluded and the same start-up operation is carried out in the second pilot burner. Once both pilots are burning, the control box IFS 258 sends an electrical sign to ignite the heat burners of the corresponding zone to start the fire test according the thermal load strategy implemented at the KS 90 programme.

### *3.3.2 Flame control*

The fulfilment of the thermal load curve is demanded by the comparison between the set-point at the KS 90 control programme and the instantaneous temperature at the control thermocouple, *TH* (Fig. 7).

The difference between theses temperatures, $\Delta\theta$, is converted in electrical information to open or close the valve RV 232; this operation adjusts the gas flow delivered to the system and consequently reduces $\Delta$. This temperature equilibrium is controlled during the whole fire test. At the end of the fire curve, the burner control unit switches off automatically and closes all the valves.

If at some point of the fire curve one of the pilot burners stops, the control box IFS 258 closes the valve RV 232 and extinguishes the burners of the corresponding zone, however if others zones exist, they continue to burn following its fire curve.

Additionally, the control system also includes a manual safety button. This button is incorporated in the control box IFS 258 and it closes the gas delivered to the system and inhibits the restart.

### 3.4 Exhaust system

In order to allow the exhaust of the smoke and combustion gases, the system presented in Fig. 8 is used. This exhaust system, fixed to the supporting structure, consists of a semi-circular steel shell around the top of the composite slab and is closed at the ends. This semi-circular steel shell drives the combustion gases through flexible steel pipes to a centrifugal ventilator that forced these gases to the outside of the Laboratory through an opening in the roof. During the test, the ventilator SP-CRMT/4-400/165.7.5 admits a maximum flow of 10460 $m^3$/h and 400ºC is the maximum allowed temperature.

### 3.5 Structural layout

The design of the experimental layout requires a reaction structure to limit the displacements at the limits of the tested structure. At the Laboratory of Structures of the University of Coimbra, the bottom of the tested structure was fixed to reinforced concrete footings that were secured in position by Dywidag bars passing through the laboratory strong floor and fixed horizontally using a steel profile connecting reinforced concrete footings to a strong wall. To restrain the horizontal movement at the top of the tested structure, it was fixed to the reaction structure and high cross-section steel beams connected the reaction structure to the strong wall. In order to avoid rotation at the top of the reaction structure and consequent errors in measurements, bracing struts were positioned between the top of the reaction structure and the top beam acting as longitudinal bracing (Fig. 9).

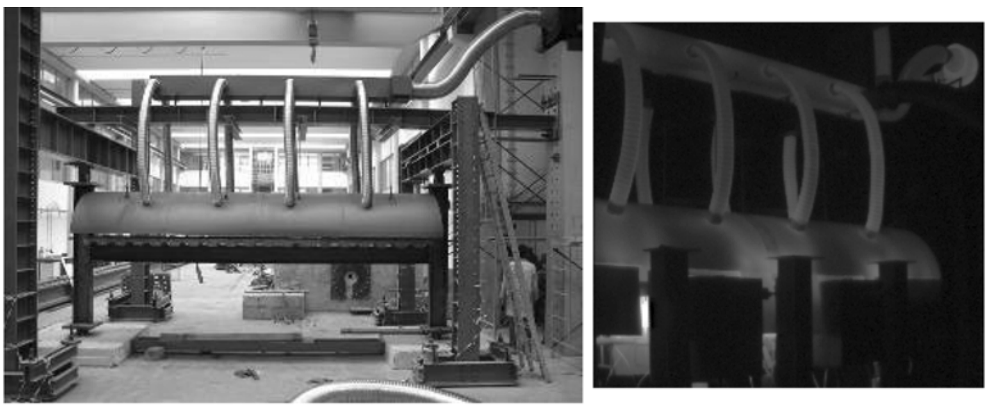

Fig. 8 General layout, including the exhaust system

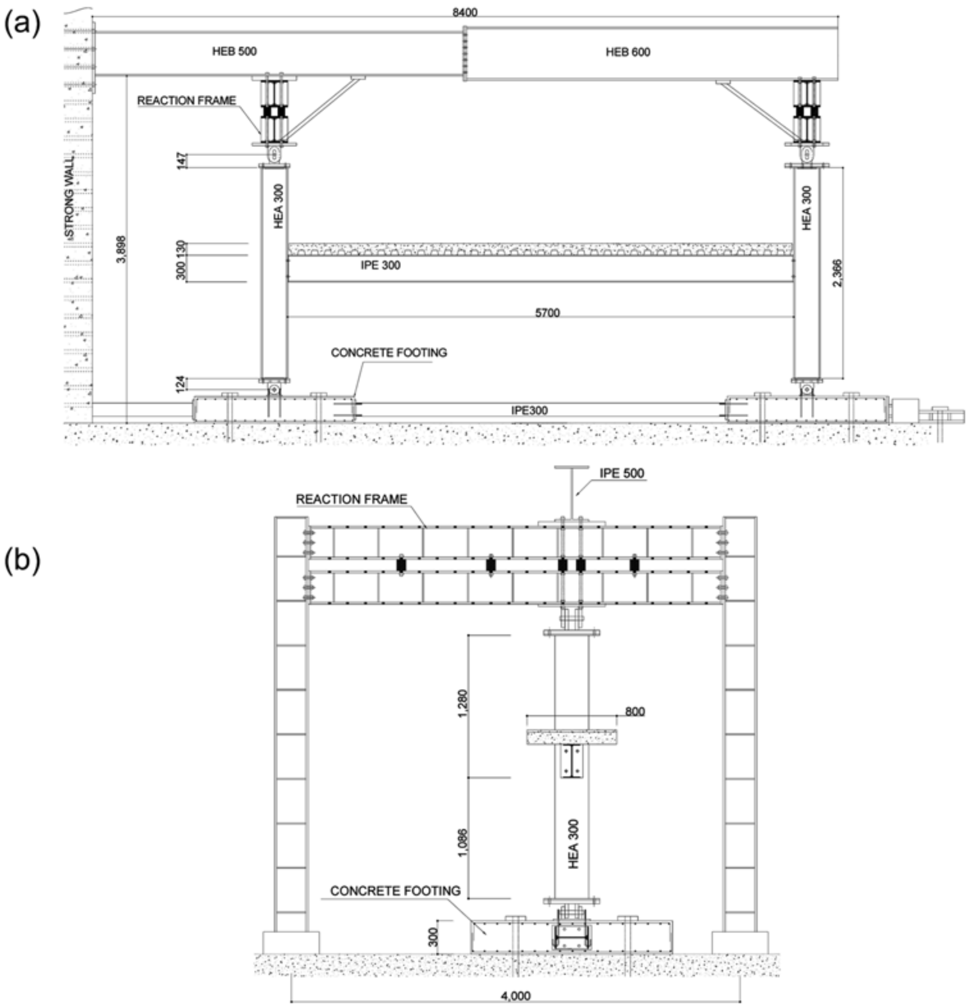


Fig. 9 General layout

### 3.6 Specimens

The modular concept of the "Natural Fire Facility" allows the testing of a wide range of structural geometries (3D, bi-dimensional, etc.) and materials (steel, concrete, timber, etc.), because of the versatility of the underlying concept.

### 3.7 Calibration of the "Natural Fire Facility"

Several preliminary heating tests using small dummy specimens were conducted i) to establish procedures for maintaining the temperature at a constant level, ii) to determine the geometry and incidence of the gas burners, iii) to determine procedures for reliable control of the heating rate with the available equipment and iv) to design the exhaust system and to assess the accuracy of the temperature measurements. Supported by a thermographic camera, Fig. 10 illustrates a study to quantify the maximum

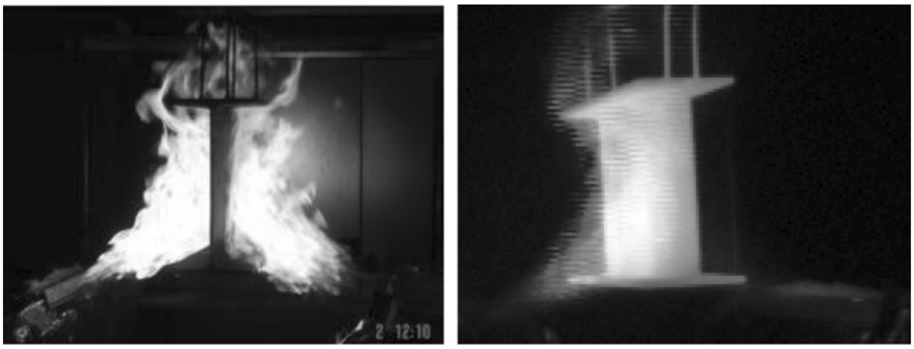

Fig. 10 Study of the maximum temperature reached during the fire

steel temperature reached during a test. These preliminaries tests showed that a local maximum temperature of 900~1,000°C was easily reached; however, it was very difficult to maintain this temperature. The semi-circular steel sheet used by the exhaust system helps to solve this problem, reducing the heat losses at the vicinity of the heated specimen.

To design the gas burners, the following requirements shall be attended: the flame incidence at the specimen shall be from the bottom and similar to the observed in a urban fire; the distance from the burner to the specimen shall be kept constant as the heated specimen deflects.

To assess the accuracy of the thermocouples used to measure the steel temperature, the dummy specimen was carefully instrumented with thermocouples positioned at the surface and inside the steel; at the same time, temperature contours were also obtained from the thermographic camera. Maximum differences of 10°C at the steel surface were measured. This was considered to be acceptable for these tests.

### *3.8 Limitations at the instrumentation of test specimens*

Thermal and mechanical results could be recorded by means of the following instrumentation: thermocouples, displacement transducers, strain gauges, load cells and thermographic cameras; however, due to direct contact with the flames or/and the elevated temperatures around the tested specimen, special conditions should be attended: In cases of long fires, thermocouples attached to the heated specimens should be protected by ceramic rods (or other thermal protection material) to eliminate the incidence of the flame that could damage the commercial protection (glass fibre), which could make the wires contact each other, consequently leading to errors of measurements (Fig. 11). Other kinds of thermocouples could be used, as for examples, protected thermocouples with a sheath of heat resistant materials, however, additional problems should be attended.

Displacement transducers are used to measure displacements and deformations of the tested specimen. Measurements should be made outside the fire zone. In our test refractory glass was used. Other alternative rigid materials with very low thermal expansion coefficient may be used. A sheaves system should be used to bring the measurements to a place with temperatures allowed by the displacement transducers.

In order to measure the elements stresses and deformations, two different types of strain gauge could be used: high temperature gauges at the zones exposed to elevated temperatures and standard gauges at the zones that remain at room temperature. High temperature gauges were not used for economic reasons.

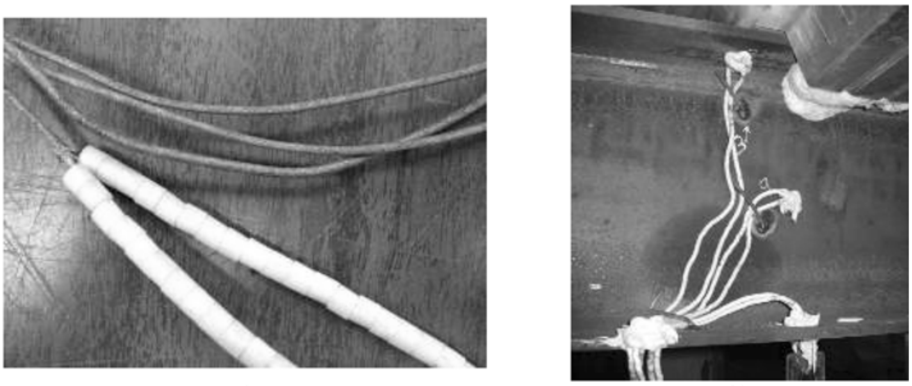

a) b)

Fig. 11 Thermocouples: a) preparation, b) application

Load cells may be used to measure forces, but only in elements that remain at room temperature.

### *3.9 Consumed energy and emissions*

Obviously, the total thermal energy required to perform a fire test depends mainly on the size of the structure to test and on the temperature-time curve applied in each zone of the structure. In this facility, the air flow that enters though the openings is enough to allow a complete combustion of the propane gas flow; so, the corresponding total thermal energy released, $E$ (kWh), assuming complete combustion and considering the low heat value of 12.9 kWh/kg for the propane gas, was:

$$E = m_{C_3H_8} \times 3 \tag{1}$$

where $m_{C_3H_8}$ (kg) is the total mass of propane gas consumed during a fire test. The average thermal power, $P$ ($kW$), applied in a fire test with a total duration of $\Delta t$ (min.), is:

$$P = \frac{E \times 60}{\Delta t} \tag{2}$$

Again, assuming complete combustion, the only pollutant emitted to the atmosphere is $CO_2$. For complete combustion of propane, the quantity of $CO_2$ emitted is 3 kg $CO_2$/kg $C_3H_8$. Thus, the total amount of $CO_2$ is:

$$m_{CO_2} = m_{C_3H_8} \times 3 \tag{3}$$

## 4 Experimental behaviour of steel sub-frame

### *4.1 Introduction*

In order to evaluate the behaviour of various types of steel joints under a natural fire and transient temperature conditions along the length of the beam, six prototypes reproducing a sub-frame of the fire compartment in the Cardington steel building (Wald *et al*. 2006) were tested. Varying beam-to-column connections representative of the most common joint types used in buildings (header plate; flush and extended end-plate and welded) were chosen to provide insight into the influence of these connection types on the behaviour of steel structures in fire.

### 4.1.1 Structural layout and test procedure

The structure consisted of two thermally insulated HEA300 cross-section columns and an unprotected IPE300 cross-section beam with 5.70 m free span, supporting a composite concrete slab. The steel grade specified for the beam and columns is S355 and the beam cross-section is class 1 for local buckling at room temperature as well as at elevated temperatures. The slab construction was of steel deck and light-weight in-situ concrete composite floor and was intended to reproduce the thermal boundary condition in typical composite frames. The steel sub-frame was supported by two reaction frames (Fig. 9) perpendicular to the plane of the frame. They provided pinned supports at the top of the columns, allowing free axial movement; the bottom of the columns was hinged and fixed to a reinforced concrete footing that was secured in position by Dywidag bars passing through the laboratory strong floor and fixed horizontally using a steel profile connecting both reinforced concrete footings.

Because lateral buckling is one of the main failure mode of steel beams with long span, which is not intended as a subject of study in this project, lateral movement at the beam's top flange was restrained at three points: i) at mid-span, ii) at 1,500 mm to the left side from the mid-span, and iii) at 1,500 mm to the right side from the mid-span. The restraint system is illustrated in Fig. 12 and it allowed vertical sliding movement.

The experimental programme comprised six tests and the varied parameter was the beam-to-column connection configuration (Table 1). Fig. 13 shows the general layout during a fire test.

The testing procedure is characterized by two different and sequential steps: step 1 - the mechanical load was applied instantaneously and measurements were recorded, step 2 - the heating unit was switched on. The mechanical loading was maintained constant and the thermal load was incremented according to the adopted fire strategy.

### 4.1.2 Loading definition

Thermal loading was applied to the beam and joints (from the beam side only). In order to prevent

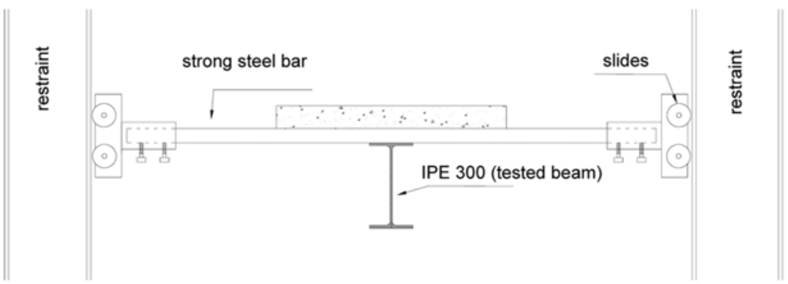


a)

b)

Fig. 12 a) Lateral restraint system, b) Detail of slide

Table 1 Test programme

| Test ID | Joint typology | End-plate dimensions (mm) and steel grade | Bolts / Weld ($a_f$, $a_w$, weld throat thickness, mm) |
|---|---|---|---|
| FJ01 | | (320 × 200 × 10), S275 | 2 bolt row M20, 8.8 |
| FJ02 | Flush end-plate | (320 × 200 × 16), S275 | 2 bolt row M20, 10.9 |
| FJ03 | | (320 × 200 × 16), S275 | 2 bolt row M20, 8.8 |
| EJ01 | Extended end-plate | (385 × 200 × 16), S275 | 3 bolt row M20, 8.8 |
| HJ01 | Header plate | (260 × 150 × 8), S275 | 4 bolt row M20, 8.8 |
| WJ01 | Welded joint | - | $a_f = a_w = 10$ |

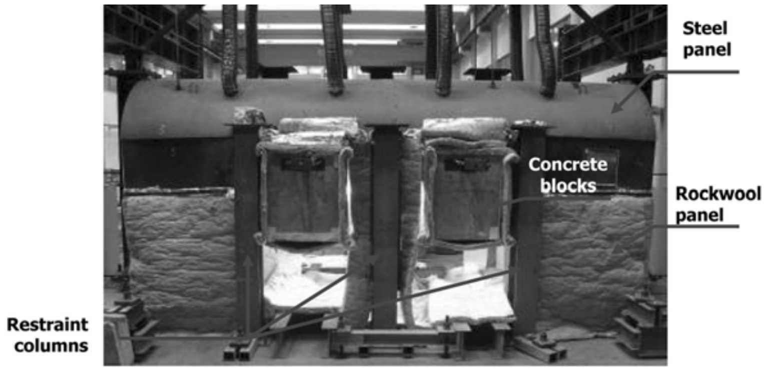


Fig. 13 General layout during a fire test

global structural instability, the columns were thermally protected by 30 mm of ceramic fibre blanket ($\lambda$ = 0.06 W/mK (200°C); $\lambda$ = 0.27 W/mK (1,000°C), where $\lambda$ denotes the thermal conductivity). Thermal loading was time dependent (heating and cooling phases) and was also variable along the beam span. The tested beams were divided into three heating zones: zone 1 (central zone) and zones 2 and 3 (end zones) (Fig. 14a). The beam temperature-time curves applied at each beam zone reproduced the values measured in a previous full-scale test (Wald *et al.* 2006) and they correspond to the measured temperatures at the beam bottom flange. Fig. 14b illustrates the adopted temperature-time curves for the 3 zones as well as the measured Cardington curve at mid-span. The first 10 min. of the full-scale fire were neglected because the corresponding temperatures were very low and difficult to reproduce (corresponding to ignition and prior to flashover in a real enclosure fire); for safety reasons, the maximum temperature applied in the tests was 900°C at the beam bottom flange (35 min < $t$ < 50 min).

In order to simulate loading conditions similar to those observed in a real structure under a fire, besides the thermal loading, mechanical loading was also considered. The mechanical loading was applied at two points of the beam top flange, 700 mm to either side of the beam mid-span. Each concentrated load was equal to 20 kN, which corresponds to a load ratio of 0.2. The load ratio is here defined as the ratio of the applied load at fire limit state ($M_{fi,d}$ = 46 kNm) to the load-carrying capacity of a simply-supported beam at room temperature ($M_{Rd}$ = 223.08 kNm based on a yield stress of 355 MPa). This mechanical loading was applied using two pairs of concrete blocks (Fig. 13).

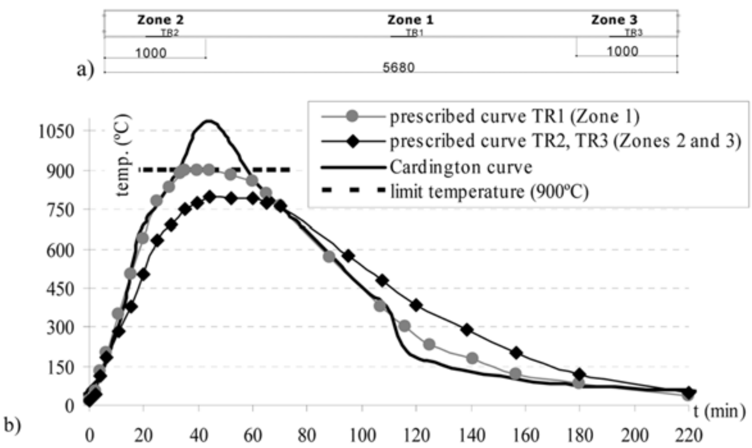


Fig. 14 Thermal loading: a) Definition of heating zones, b) Time-temperature curves

## 4.2 Results

### 4.2.1 Efficiency of the natural fire facility

Fig. 15 compares the adopted fire curves (control system) with the temperatures measured at the beam reference points (TR1, TR2 and TR3) for test EJ01. Good agreement was observed during both the heating and cooling phases. Similar results were observed for the other five tests.

### 4.2.2 Beam temperatures

Fig. 16 depicts the temperature distribution across the beam mid-span cross section for test EJ01. Temperature measurements at mid-span of the beams were taken in the bottom flange (both sides), web and top flange. During the heating phase, the web and bottom flange temperatures are quite similar, despite the fact that the flames surround the bottom flange earlier, the reduced web thickness allowing a faster temperature increase. In the cooling phase, the web temperature decreased faster than the bottom flange temperature for the two following reasons: i) the reduced thickness corresponds to a lower thermal inertia and ii) during this phase, the length of flames reduces, and, from a certain moment in

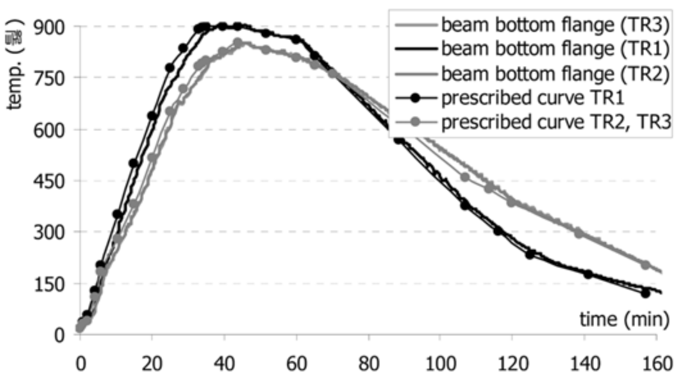


Fig. 15 Beam temperature versus adopted fire curves (test EJ01)

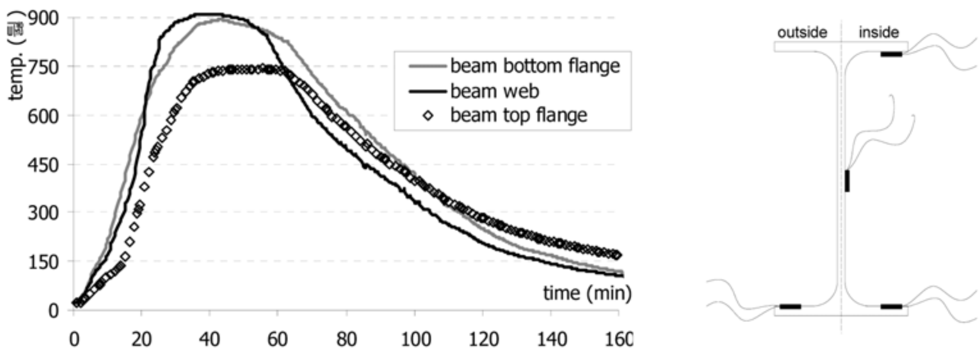


Fig. 16 Temperature curves across the beam mid-span

time onwards, they only surround the bottom flange. Because of shielding by the concrete slab that reduces the heat transfer, the top flange showed: i) the lowest temperature during the heating phase with a maximum temperature of about 743°C, ii) slower cooling down, and iii) the maximum top flange temperature was recorded during the cooling phase. Fig. 17, obtained using a thermographic camera, illustrates the temperature distribution in the central zone of the beam during the heating phase.

Table 2 summarises the temperatures across the depth of the beams; for each test, three different cross-sections were measured: a) mid-span, b) at 1,650 mm to the Z3 side from the mid-span, c) at 1,650 mm to the Z2 side from the mid-span. All tests showed similar temperature development during the fire. The average coefficient of variation, *COV*, is about 4.2%, while the maximum coefficient of variation does not exceed 12%.

### *4.2.3 Joint temperature*

Another goal of this facility was the possibility to divide the tested structure in several zones and to specify individual thermal load strategies to each zone. Fig. 18 compares the temperature-time variation across the depth of the beam 200 mm away from the connection Z3 with the bottom flange temperature at mid-span (test EJ01). During the heating phase, the joint temperature was significantly lower than the mid-span bottom flange, which is usually the critical element that defines the limiting temperature of the beam; in contrast, the cooling down in the joint was slower, in accordance with what happens in a

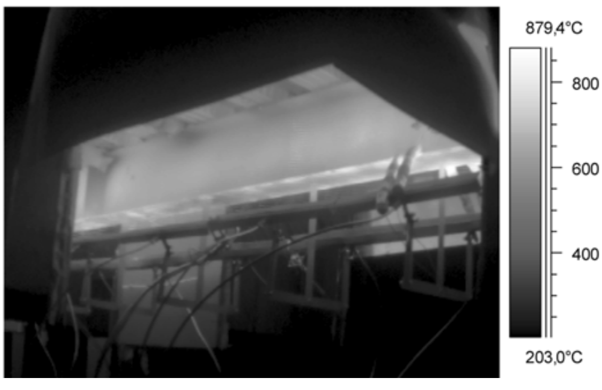


Fig. 17 Thermographic image of temperature in the beam during the heating phase

Table 2 Temperatures at beam mid-span

| | | Temperature | | | | | | | |
|---|---|---|---|---|---|---|---|---|---|
| | | 15 min. | 25 min. | 40 min. | 50 min. | 60 min. | 70 min. | 80 min. | 150 min. |
| | bottom flange | 454 | 711 | 877 | 878 | 815 | 721 | 619 | 171 |
| FJ01 | web | 346 | 694 | 878 | 873 | 801 | 669 | 538 | 144 |
| | top flange | 253 | 505 | 770 | 813 | 780 | 669 | 566 | 226 |
| | bottom flange | 493 | 730 | 896 | 886 | 867 | 753 | 647 | 183 |
| FJ02 | web | 400 | 725 | 872 | 864 | 847 | 645 | 552 | 150 |
| | top flange | (a) | (a) | (a) | (a) | (a) | (a) | (a) | (a) |
| | bottom flange | 499 | 740 | 911 | 908 | 867 | 774 | 680 | 178 |
| FJ03 | web | 423 | 730 | 871 | 852 | 792 | 680 | 568 | 162 |
| | top flange | 309 | 588 | 797 | 826 | 810 | 735 | 629 | 206 |
| | bottom flange | 452 | 727 | 890 | 898 | 845 | 710 | 605 | 152 |
| EJ01 | web | 374 | 774 | 882 | 867 | 771 | 623 | 518 | 133 |
| | top flange | 231 | 555 | 763 | 785 | 769 | 677 | 571 | 178 |
| | bottom flange | 489 | 733 | 882 | (b) | (b) | (b) | (b) | (b) |
| HJ01 | web | 394 | 718 | 845 | (b) | (b) | (b) | (b) | (b) |
| | top flange | 245 | 554 | 743 | (b) | (b) | (b) | (b) | (b) |
| | bottom flange | 478 | 732 | 904 | 914 | 888 | 784 | 679 | 166 |
| WJ01 | web | 423 | 726 | 868 | 866 | 829 | 719 | 599 | 158 |
| | top flange | 326 | 613 | 787 | 813 | 815 | 733 | 614 | 208 |
| | bottom flange | 477 | 729 | 893 | 897 | 857 | 748 | 646 | 170 |
| Average | web | 393 | 728 | 869 | 864 | 808 | 667 | 555 | 149 |
| | top flange | 273 | 563 | 772 | 809 | 793 | 704 | 595 | 204 |
| | bottom flange | 4.2 | 1.3 | 1.4 | 1.5 | 2.9 | 3.9 | 4.7 | 6.4 |
| *COV* (%) | web | 7.5 | 3.5 | 1.5 | 0.8 | 3.3 | 4.9 | 4.9 | 7.1 |
| | top flange | 12 | 7.1 | 2.8 | 1.0 | 1.8 | 3.5 | 3.7 | 7.7 |

(a) not measured, (b) beam failure

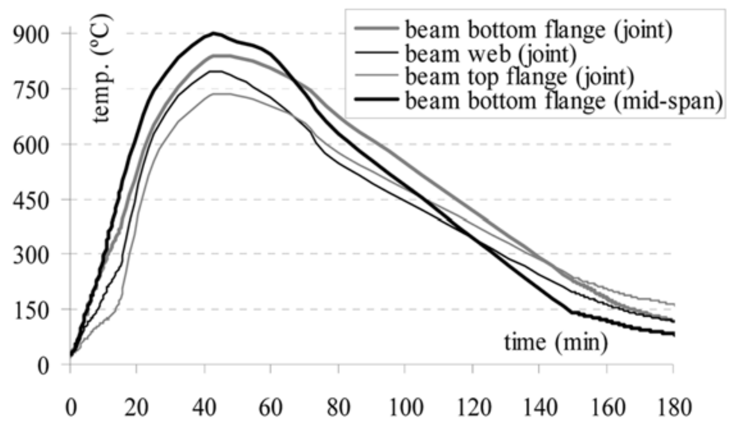


Fig. 18 Temperature curves across the depth of the beam 200 *mm* away from the connection Z3 (test EJ01)

real fire situation (Wald *et al.* 2006b). The maximum temperature near the joints was measured in the bottom flange and corresponded to about 90% of the maximum temperature at mid-span.

Table 3 summarises the temperatures across the depth of the beams 200 mm away from the face of the columns in zones Z2 and Z3. All tests showed similar temperature development during the fire. The average coefficient of variation is about 3.6%, while the maximum coefficient of variation does not exceed 9.8%.

Fig. 19 compares the temperature curves for the various connection elements of joints in zone Z3 (test EJ01). Measurements were made for each bolt-row as follows: i) in the bolt (beam side; ii) in the bolt shank under the nut (column side), and iii) in the end-plate at the same level of the bolt. Again, in the heating phase, the connection temperature was significantly lower than the remote bottom flange at mid-span; in contrast, the cooling down in the joint elements was slower, because of: i) shielding by the

Table 3 Temperatures at beam near the connection (200 mm).

| | | Temperature | | | | | | | |
|---|---|---|---|---|---|---|---|---|---|
| | | 15 min. | 25 min. | 40 min. | 50 min. | 60 min. | 70 min. | 80 min. | 150 min. |
| FJ01 | bottom flange | 326 | 563 | 778 | 821 | 793 | 745 | 670 | 242 |
| | web | 290 | 587 | 788 | 790 | 735 | 635 | 540 | 206 |
| | top flange | 199 | 424 | 703 | 752 | 742 | 655 | 569 | 247 |
| FJ02 | bottom flange | 359 | 612 | 751 | 784 | 783 | 748 | 677 | 234 |
| | web | 269 | 620 | 738 | 752 | 751 | 702 | 590 | 178 |
| | top flange | 195 | 453 | 666 | 672 | 687 | 687 | 607 | 256 |
| FJ03 | bottom flange | 352 | 643 | 842 | 841 | 804 | 766 | 701 | 249 |
| | web | 298 | 599 | 783 | 782 | 731 | 670 | 589 | 215 |
| | top flange | 214 | 520 | 746 | 752 | 713 | 664 | 596 | 258 |
| EJ01 | bottom flange | 379 | 660 | 841 | 847 | 813 | 761 | 686 | 236 |
| | web | 301 | 632 | 811 | 798 | 745 | 674 | 577 | 200 |
| | top flange | 202 | 555 | 763 | 764 | 720 | 670 | 593 | 241 |
| HJ01 | bottom flange | 371 | 638 | 827 | (b) | (b) | (b) | (b) | (b) |
| | web | 269 | 560 | 737 | (b) | (b) | (b) | (b) | (b) |
| | top flange | 206 | 470 | 681 | (b) | (b) | (b) | (b) | (b) |
| WJ01 | bottom flange | 363 | 615 | 822 | 836 | 798 | 753 | 684 | 236 |
| | web | 300 | 578 | 788 | 786 | 750 | 685 | 585 | 203 |
| | top flange | 191 | 472 | 731 | 750 | 715 | 674 | 592 | 246 |
| Average | bottom flange | 358 | 622 | 810 | 826 | 798 | 754 | 683 | 239 |
| | web | 288 | 596 | 774 | 781 | 742 | 673 | 576 | 200 |
| | top flange | 201 | 482 | 715 | 738 | 715 | 670 | 591 | 249 |
| *COV* (%) | bottom flange | 5.2 | 6.0 | 5.1 | 2.6 | 1.1 | 1.2 | 1.6 | 2.2 |
| | web | 5.2 | 4.5 | 3.9 | 2.0 | 1.1 | 3.3 | 3.2 | 6.1 |
| | top flange | 4.1 | 9.8 | 5.3 | 4.5 | 2.4 | 1.6 | 2.1 | 2.6 |

(b) beam failure

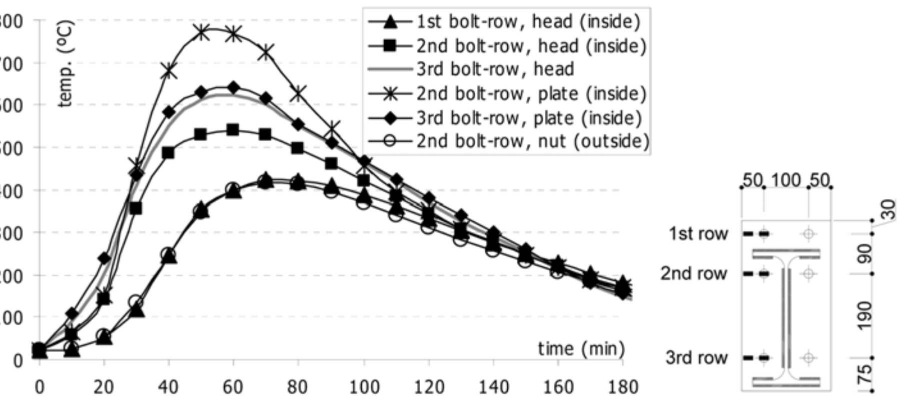


Fig. 19 Temperature within the joint Z3 (test EJ01)

adjacent cold column, ii) concentration of mass in the connection elements, and, iii) the different thermal loading applied at the joints section. The maximum temperature at the connection is thus reached during the cooling phase. The first bolt row from the top was significantly cooler than the lower bolts, because of shielding by the adjacent slab. The end-plate temperature was quite similar to that of the bolt head at the same level. Exception is made at the level of the second bolt-row; in this case, the flames engaged the plate thermocouple more than the bolt head thermocouple and the end-plate received more heat than the bolt head. This measurement should not be considered as representative of the average plate temperature at this level. Temperature gradient along the bolts was also measured: the maximum temperature in the head of the third bolt-row was about 150~200ºC higher than the corresponding shank; a maximum temperature of about 400ºC was measured in the shanks. For the first bolt-row, a difference of about 60ºC on the maximum temperature is observed; this difference could be due to the shielding effect by the concrete slab. The effect of the heat transfer by conduction on the joint element is also evident: the bolt heads and plate heat up first, followed by the corresponding shanks.

### *4.2.4 Structural deformation*

Fig. 20 depicts the evolution of the beams mid-span deflection during the fire. The possibility to quantify the mechanical behaviour of a restrained structure during the cooling phase was, perhaps, the major goal of this facility. Most of the beams were able to sustain the load with very deflections up to 10 min ($\theta_0 < 150$ºC); during this stage, the deflection was mainly due to the mechanical loading. Beyond that, due to the loss of stiffness, the mid-span deflection increased gradually. Beyond 20 min, a further rise in temperature ($\theta_0 > 550$ºC) led to a progressive run-way of the beam deflection as the loss of stiffness and strength accelerated. In the case of tests FJ02, EJ01 and WJ01, a maximum deflection of 375 mm was approximately reached (these values were measured already during the cooling phase). For the PJ01 test, Z3 joint collapsed during the heating phase of the fire ($\theta_0 = 900$ºC) as a result of the run-way deflection at high temperatures ($\delta_{beam} = 393$ mm). Once the cooling phase started, the heated beams began to recover strength and stiffness from an inelastic state, together with a reduction of thermal strains. This induced tensile axial forces and the reversal of the deflection. Because of the limited range of the displacement transducers (400 mm), FJ01 curve was incomplete; however, a maximum deflection of 428 mm was measured at the end of the fire. Fig. 21 shows the deformed structure at the end of the test.

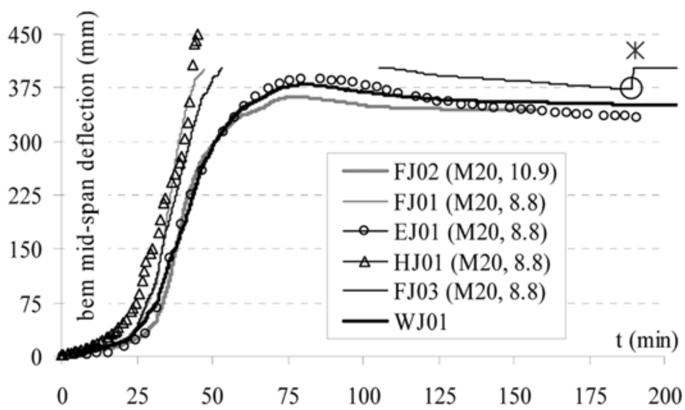


Fig. 20 Mid-span deflection of the beam

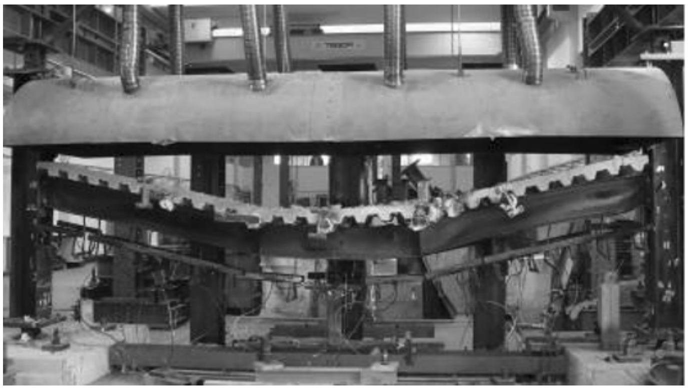

Fig. 21 Deformed structure after test FJ01

#### *4.2.5 Failure modes*

The first fire tests performed at a steel structure, with the aim of studying the joint behaviour, showed that the modes of failure of these joints were qualitatively similar to those observed at room temperature (Leston-Jones *et al.* 1997). With this "Natural Fire Facility", with mechanical and thermal conditions similar to those observed in a real steel structure under a fire, it was observed that joint failure modes are quite distinct from those observed at room temperature. The following paragraph will describe some of the main failure modes observed on the tested joints: in the end-plate joints and during the heating phase, local buckling on the bottom flange and shear failure at the web were noticed. At the same time, and due to the large joint bending moment, end-plate deformation at the top developed and in some joints, the weld on the top flange was broken (Fig. 22a). During cooling and due to the large tensile forces that developed during this phase, minor cracks on the weld at the bottom flange were observed together with bolt failure in some joints (Fig. 22b).

In the header plate joint, during the heating phase, local buckling on the bottom flange was observed; shear failure at the beam web was insignificant. At the maximum joint temperature (850ºC), the end-plate broke along both beam web welds (joint Z3), due to the considerable rotation before the beam and column flange came into contact (Fig. 23a), rapidly the beam suffered a large deflection and shear

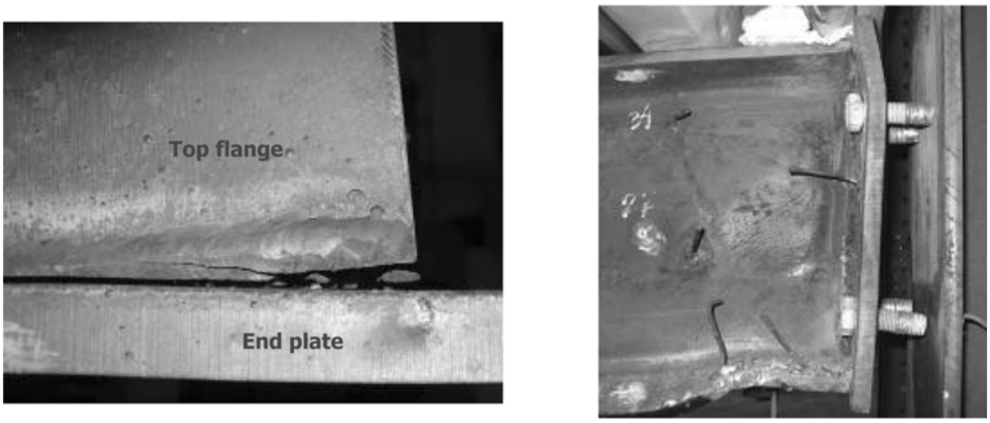


Fig. 22 a) Weld fracture (view from the top of the beam) and b) joint after failure (test FJ03)

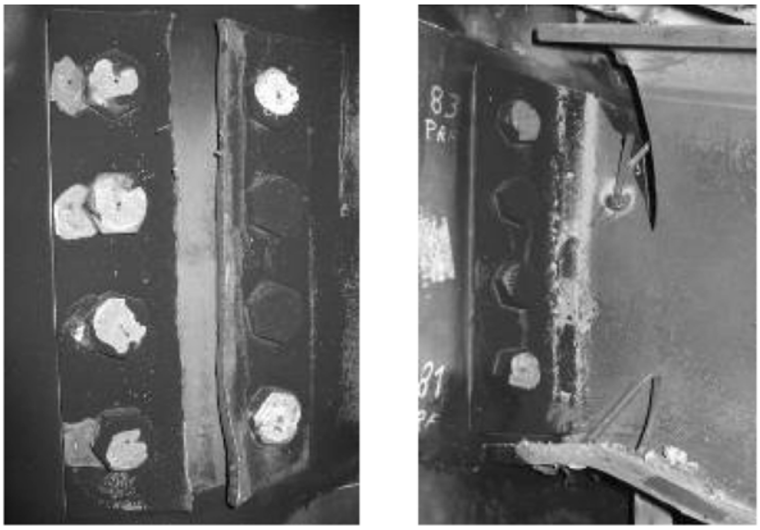

Fig. 23 a) End-plate failure (joint Z2) and b) beam failure (joint Z3) at test HJ01

forces were developed near the joint Z2, leading to beam rupture (Fig. 23b). No damage to the bolts was observed. In the welded joint, local buckling on the bottom flange was observed; shear failure at the beam web was minor and no damage to the welds was observed.

Furthermore, other failure modes were observed in the beam and in the concrete slab: shear buckling of the beam web near the load points, bursting of the concrete slab; large cracks on the concrete slab due to the separation of the shear studs from the concrete slab, major cracks perpendicular to the slab that occurred as a result of the beam and joints deformation. Due to the considerable size of the columns, column deformations are irrelevant.

### *4.3 Consumed energy and emissions during the test*

In this fire test and for the conditions described in § 4.1.1, the total mass of propane gas consumed was $m_{C_3H_8} = 135\ \text{kg}$. This value was obtained by weighting the gas reservoirs before and after the test, so, the corresponding total thermal energy released was $E = 1741.5$ kWh. As the total fire duration was 220 min. (approximately), the averaged thermal power applied was $P = 474.9$ kW, and the total amount of $CO_2$ emitted to the atmosphere was $m_{CO_2} = 405\ \text{kg}$.

## 5. Conclusions

The "Natural Fire Facility" developed within this project allows the controlled fire testing of a full-size steel sub-frame under transient fire conditions (in time and in space). The modular concept of this experimental installation allows its use for a wide range of structures and materials, reproducing real fire conditions very successfully.

The experimental results for the six tests show a clear influence of the joint typologies on the overall response of the sub-frame. The tests demonstrated the appearance of large tensile forces and the reversal of bending moment during the cooling phase, already shown numerically by the authors (Santiago *et al.* 2003). They also demonstrated that these forces may result in failure of the joint, as was already postulated by the authors in previous works (Simões da Silva *et al.* 2005). Finally, these test results give clear guidance on how to propose design guidance to avoid failure of the joints under fire loading, in the framework of the component method under fire conditions (Simões da Silva *et al.* 2002), a task that is currently being actively developed by the authors.

## Acknowledgement

Financial support from the Portuguese Ministry of Science and Higher Education (*Ministério da Ciência e Ensino Superior*) under contract grant POCI/ECM/55783/2004 is gratefully acknowledged. Propane gas from GALP S.A. and technical support from CHAMA S.A. is also recognized.

## References

ECSC project 7210, 2000 "Natural fire safety concept. Full Scale tests, Implementation in the Eurocodes and Development of an User-friendly Design Tool". ECSC project 7210-PA/PB/PC/PD/PE/PF/PR-060, 1997-2000.

Leston-Jones, L.C., Burgess, I.W., Lennon, T., Plank, R.J., "Elevated-temperature moment-rotation tests on steelwork connections", *Proc. Instn Civil Engrs, Structures & Buildings*, **122**, pp. 410-419, 1997.

Liu, T.C.H., Fahad, M.K. and Davies, J.M., "Experimental investigation of behaviour of axial restrained steel beams in fire", *J. Constr. Steel Res.*, **58**, 1211-1230, 2002.

Santiago, A., Simões da Silva, L. and Vila Real, P., "Effect of cooling on the behaviour of a steel beam under fire loading including the end joint response", *Proceedings of 9th International Conference on Civil and Structural Engineering Computing*, Egmond-aan-Zee, Nederlands, September 2-4, 2003.

Simões da Silva, L., Santiago, A. and Vila Real, P. "A component model for the behaviour of steel joint at elevated temperatures", *J. Constr. Steel Res.* **57**(11), pp. 1169-1195, 2002.

Simões da Silva, L. Santiago, A., Vila Real, P. and Moore, D.B., "Behaviour of steel joints under fire loading", *Steel Compos. Struct.* **6**, 485–513, 2005.

Trinks W., Mawhinney, M.H., Shannon, R.A., Reed, R.J and Garvey, J.R., *Industrial Furnaces*, 6th edition, John Wiley & Sons, Inc., 2004.

Wald, F, Simões da Silva, L., Moore, D., Lennon, T., Chladna, M., Santiago, A., Benes, M., and Borges, L.,

"Experimental behaviour of a steel structure under natural fire", *Fire Safety J.,* **4**1(7), pp. 509-522, 2006.
Wang, Y.C., *Steel & Comp. Struct – behaviour and design for fire safety*, Spon Press, London, 2002.
Vila real, P.M.M., Piloto, P.A.G. and Franssen, J.-M.; "A new proposal of a simple model for lateral-torsional buckling of unrestrained steel i-beams in case of fire: experimental and numerical validation". *J. Constr. Steel Res.*, **59**(2), 179-199, 2003.

*YW*